CrossMark

ORIGINAL PAPER

Spatial distribution patterns of ascidians (Ascidiacea: Tunicata) on the continental shelves off the northern Antarctic Peninsula

Alexandra Segelken-Voigt[1,2] · Astrid Bracher[2,3] · Boris Dorschel[2] ·
Julian Gutt[2] · Wilma Huneke[2] · Heike Link[4] · Dieter Piepenburg[2,4]

Abstract Ascidians (Ascidiacea: Tunicata) are sessile suspension feeders that represent dominant epifaunal components of the Southern Ocean shelf benthos and play a significant role in the pelagic–benthic coupling. Here, we report the results of a first study on the relationship between the distribution patterns of eight common and/or abundant (putative) ascidian species, and environmental drivers in the waters off the northern Antarctic Peninsula. During RV *Polarstern* cruise XXIX/3 (PS81) in January–March 2013, we used seabed imaging surveys along 28 photographic transects of 2 km length each at water depths from 70 to 770 m in three regions (northwestern Weddell Sea, southern Bransfield Strait and southern Drake Passage), differing in their general environmental setting, primarily oceanographic characteristics and sea-ice dynamics, to comparatively analyze the spatial patterns in the abundance of the selected ascidians, reliably to be identified in the photographs, at three nested spatial scales. At a regional (100-km) scale, the ascidian assemblages of the Weddell Sea differed significantly from those of the other two regions, whereas at an intermediate 10-km scale no such differences were detected among habitat types (bank, upper slope, slope, deep/canyon) on the shelf and at the shelf break within each region. These spatial patterns were superimposed by a marked small-scale (10-m) patchiness of ascidian distribution within the 2-km-long transects. Among the environmental variables considered in our study, a combination of water-mass characteristics, sea-ice dynamics (approximated by 5-year averages in sea-ice cover in the region of or surrounding the photographic stations), as well as the seabed ruggedness, was identified as explaining best the distribution patterns of the ascidians.

This article belongs to the special issue on "High environmental variability and steep biological gradients in the waters off the northern Antarctic Peninsula," coordinated by Julian Gutt, Bruno David and Enrique Isla.

✉ Alexandra Segelken-Voigt
alexandra.segelken.voigt@uni-oldenburg.de

[1] Carl von Ossietzky University of Oldenburg, Ammerländer Heerstraße 114 - 118, 26129 Oldenburg, Germany

[2] Alfred Wegener Institute, Helmholtz Centre for Polar and Marine Research, Am Handelshafen 12, 27570 Bremerhaven, Germany

[3] Institute of Environmental Physics, University of Bremen, Otto-Hahn-Allee 1, 28359 Bremen, Germany

[4] Institute for Ecosystem Research, University of Kiel, Duesternbrooker Weg 20, 24105 Kiel, Germany

Keywords Environmental drivers · Spatial scales · Photographic survey · Bottom topography · Macrobenthos · Southern Ocean

Introduction

A unique fauna has evolved on the continental shelves of the Southern Ocean in the past 25 million years with regional peculiarities, related to differences in ecological conditions in terms of hydrography, food supply and sea-ice dynamics (Vaughan et al. 2003; Clarke et al. 2009; Jerosch et al. 2015; Moreau et al. 2015). In this time, the Antarctic Peninsula had developed to a region with the highest environmental heterogeneity in the Southern Ocean and to a benthic biodiversity hot spot (Walther et al. 2002). During the past five decades, this region became one of the

fastest warming regions on Earth which resulted in altered sea-ice dynamics, disintegration of ice shelves and retreat of glaciers (Vaughan et al. 2003; Cook et al. 2005). This long-term and short-term temporal variability, in combination with a small-scale and large-scale spatial patchiness of environmental factors, has direct and indirect impacts on benthic species due to their limited physiological tolerance and relatively high degree of environmental adaptation (Barnes et al. 2009; Peck et al. 2009).

Ascidians (Ascidiacea: Tunicata) represent dominant epifaunal components of the Southern Ocean shelf benthos. In general, they are known to respond fast to environmental changes by immediate and rapid recruitment and population growth, but also by high local mortality (Kowalke 1999; Newton et al. 2007; Primo and Vázquez 2009, 2014; Sahade et al. 2015). As suspension feeders, they potentially reflect changes in the pelagic–benthic coupling more directly than scavengers and predators. For this reason, ascidians are particularly suited as indicators for ecological differences in benthic habitats, between different regions and as an early warning system for environmental changes.

The Antarctic ascidian fauna has been studied in some regions of the Southern Ocean by local SCUBA dives or by trawls, e.g., off the Shetland Archipelago and in the Weddell Sea (Millar 1960; Tatián et al. 1998a, b; Ramos-Esplá et al. 2005; Tatián et al. 2005; Primo and Vázquez 2007). In a review and the presence-/absence-based circumpolar community analysis, Primo and Vázquez (2009) listed 100 species, of which 74 were recorded from the Antarctic Peninsula area and Weddell Sea. Here, we report the results of a multi-scale field study on the distribution patterns of eight common and/or abundant ascidian species found off the northern Antarctic Peninsula, which has been carried out for the first time by means of photographic transects of the seafloor. This noninvasive technique is highly efficient for benthic studies at intermediate and large spatial scales if stations cover large regions and several habitats (Gutt and Starmans 1998; Starmans et al. 1999). Photographic transects provide results on the abundance and distribution patterns at small spatial scales. This information is important to evaluate the representativeness of station-based data for a large-scale approach and cannot be detected by trawling or with grabs (Piepenburg et al. 1997; Gutt and Starmans 1998; Starmans et al. 1999).

The overarching aim of this investigation was to study ascidians as an indicator for spatial environmental variability, to determine for the first time ecological driving forces of their regional distribution and to provide a reproducible baseline for future studies on the impact of environmental changes. With this background, we used a nested sampling design including large, intermediate and small scales to test the following three hypotheses: (1a) At a large-scale (100-km) level, assemblages of ascidians differ in distribution, composition and abundance between the three regions northwestern Weddell Sea, southern Bransfield Strait and southern Drake Passage, (1b) variation in major environmental parameters explains these differences, such as water masses and sea-ice coverage, which effect primary production providing food for the benthos. (2) At an intermediate-scale (10-km) level, habitats within each of the regions differ in their ascidian assemblages. All three regions of investigation were characterized by complex shelf bottom topography, assumed to provide distinct habitats with different environmental settings. Such key habitats and ecosystems are often hot spots of enhanced biodiversity and biomass (Ramirez-Llodra et al. 2010). (3) At a small-scale (within-transect, 10-m) level, the distribution of ascidians was hypothesized to reflect specific small-scale environmental differences and gradients, as it is also known from other benthic taxa in both polar marine ecosystems (Gutt and Starmans 2003).

Materials and methods

Sampling

Seabed images were taken during cruise ANT-XXIX/3 (PS81) of RV *Polarstern* in austral summer (January–March) 2013, using the Ocean Floor Observation System (OFOS), see Gutt (2013) for a cruise report. All images, including metadata, are available in the data repository PANGAEA (www.pangaea.de; see DOIs for photographs ranging from 10.1594/PANGAEA.818400 to 10.1594/PANGAEA.818515 and 10.1594/PANGAEA.849291 (Segelken-Voigt et al. 2015) for supplementary data).

The setup and mode of deployment of the OFOS was similar to that described by Bergmann and Klages (2012). OFOS is a surface-powered gear equipped with a downward-looking, high-resolution (21 MPix), wide-angle camera system (CANON® EOS 1Ds Mark III). OFOS was vertically lowered over the side of the ship until it hovers 1.5 m above the seabed. Then, it was towed beside the slowly sailing ship at a speed of 0.5 kn (approximately 0.25 m s^{-1}). During the casts, OFOS was kept hanging at the preferred height above the seafloor by means of a live video feed and occasional minor height adjustments with the winch, depending on small-scale bathymetric variations in seabed morphology. Information on water depth and height above the seafloor was continuously recorded by means of OFOS-mounted sensors. Experience from previous expeditions, during which a Posidonia system has been used for underwater navigation of the OFOS, has shown that at a low tow speed of 0.25 m s^{-1} the OFOS is constantly hanging almost directly below the side of the ship

during the entire cast, with a deviation that is within the precision of the ship-based global positioning system (GPS; ±10 m). The observations that during the entire duration of the casts the inclination of the fiber-optic cable connecting the OFOS and the ship continues to be vertical and that the length of the cable paid out does not exceed the water depth provided further evidence for the validity of this assumption. Therefore, we used the ship's GPS position to approximate the position of the OFOS at depth (note: the position of the crane derrick used to deploy the OFOS is 27.2 m behind and 11.9 m to starboard of the ship's GPS reference point). Three lasers, which are placed beside the camera to emit parallel beams, project light points arranged as an equilateral triangle with a side length of 50 cm in each photograph, thus providing a scale that can be used to calculate the photographed area in each image. In automatic mode, a seabed photograph was taken every 30 s to obtain series of several hundred images along transects of up to 4 km length each. With a ship speed of 0.5 kn, the average distance between the seabed images was approximately 5 m. Each transect was carried out within a narrow depth range, with the exception at the Nachtigaller Shoal in the Weddell Sea.

A total of 28 OFOS stations were considered in our study on ascidian distribution patterns, which were situated in three regions off the Antarctic Peninsula between 61°S and 64°S: the northwestern Weddell Sea off Joinville Island, the southern Bransfield Strait and the southern Drake Passage west of South Shetland Islands (Fig. 1; Online Resource 1). These regions are especially well suited for a comparative ecological study with a biogeographical background, since they are characterized by different environmental conditions in terms of sea-ice coverage, current regime and food supply (Sievers 1982; Lockhart and Jones 2008; Clarke et al. 2009; Dorschel et al. 2015). Within these regions, regional habitat blocks were selected, which comprised bathymetric intermediate-scale shelf–canyon gradients (Table 1). In the Bransfield Strait, such bottom topography structures were most obvious, and three distinct habitat blocks were sampled. Within the blocks, single stations were associated with the following defined, primarily depth-related habitats: bank, upper slope, slope and deep/canyon. In the Drake Passage, where the bottom topography was similar, albeit less pronounced as in the Bransfield Strait, also three habitat blocks were sampled. In the Weddell Sea, stations were selected to cover a range of habitats that are as comparable as possible to those sampled in the Bransfield Strait. Downslope OFOS transects (=stations) at the Nachtigaller Shoal covered more than one of the above-mentioned habitats. Therefore, these transects were split into sections to be attributed to the four habitats. For statistical analyses, the habitats of all regions were classified in the factor 'Depth'

that contains the two levels 'shallow' (merged from 'bank' and 'upper slope') and 'deep' (merged from 'slope' and 'deep/canyon') since not all habitats were equally distributed in all regions. For convenience throughout the manuscript, the stations will be abbreviated by using their region initials (Table 1: Weddell Sea = WS; Bransfield Strait = BS; Drake Passage = DP), habitat-block labels (east = E; central = C; west = W; Joinville North = JN; Joinville East = JE; Dundee Ville = DU; Erebus and Terror = ET; Nachtigaller Shoal = NG) and the initials of the habitats (bank = B; upper slope = U; slope = S; deep/canyon = D). Ship's positions are provided for start, center and end of each standardized 2-km-long section of the entire transects (Online Resource 1), assuming that the small difference between the ship's and OFOS's positions is negligible in the context of our analysis (see above). Transect lengths were calculated as the sum of distances between successive photographs selected for analysis.

Photographic analysis

Firstly, photographs were discarded that were out of focus, with heights above seabed of <1.5 m and >2.5 m and/or of low quality due to other reasons, e.g., suspended sediment in the water. Based on the altitude of the OFOS above the seabed measured for each photograph by an altimeter, the analyzed images were calculated to represent an average area of the seabed of 4.76 m^2 ($\sigma = 2.49$ m^2). Then, standardized 2-km sections were selected from the total transects by randomly determining a first photograph at a minimum distance of 2 km to the transect end. The end of this 2-km section was marked by the last photograph. Additional 98 (from approximately 250) pictures were randomly selected between the first and last photograph. Transects at Nachtigaller Shoal included multiple depths (stations 185, 186, 188, 189) and were consequently divided into habitat-specific sections: bank, upper slope, slope and deep/canyon. Habitat-specific sections from adjacent transects were combined, so that the number of photographs or combined transect length was comparable to transects from the other locations, e.g., a combined transect included 100 photographs. Ascidians were counted and classified to putative species level, using specific morphological characteristics provided by Tatián et al. (1998b), Sieg and Wägele (1990) and the Ascidiacea World Database (Shenkar et al. 2015), as well as comparison with ascidian specimens collected from trawl catches carried out at the same or nearby stations. Colonial specimens were counted as single individuals. Counts of ascidians were standardized to abundance values (ind. m^{-2}). Averages and standard deviations of abundances were calculated across transects.
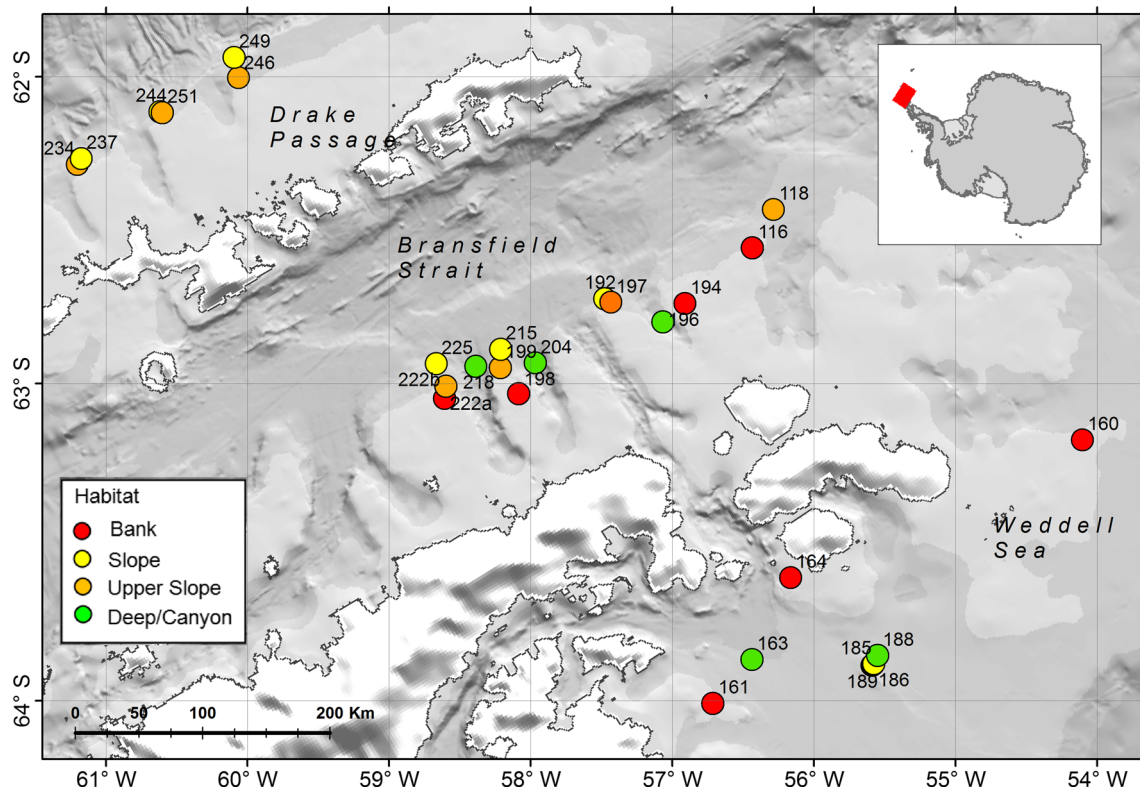
Fig. 1 Map of the location of stations where seabed photographs were taken along 2-km-long transects in the three regions (Weddell Sea, Bransfield Strait and Drake Passage) during cruise ANT-XXIX/3 of RV *Polarstern* in January–March 2013. *Numbers* are stations number; colors represent the different benthic habitats covered in the survey: *red* bank, *yellow* slope, *orange* upper slope, *green* deep/canyon. Transects at Nachtigaller Shoal included multiple depths (stations 185, 186, 188, 189) and were consequently divided into habitat-specific sections. See Online Resource 1 for station list. (Color figure online)

Environmental data

Oceanographic data on sea-water temperature, salinity and oxygen concentration were obtained by means of a CTD, using the closest CTD measurement above the bottom. The sensors had an accuracy of 2 mK for temperature, 0.002 psu for salinity and 34 μm kg^{-1} for oxygen concentration (Huneke et al. pers. comm.).

Sea-ice concentrations were provided by satellite data (Advanced Microwave Scanning Radiometer-Earth Observing System (AMSR-E), Advanced Microwave Scanning Radiometer-2 (AMSR2) and Special Sensor Microwave/Imagers (SSMIS) 89/91 GHz), averaged over 5 years using the ASI algorithm (Spreen et al. 2008) from daily observations with 6.25-km spatial resolution between January 2003 and March 2013. SSMIS data have lower resolution than the grid and were only used in the case no AMSR* instrument was operational (between October 1, 2011, and July 24, 2012). The uncertainty for the AMSR-E SIC is 25% for 0 % and 5.7 % for 100 % SIC (Spreen et al. 2008).

Phytoplankton chlorophyll-*a* (Chl-*a*) concentrations were derived from the merged daily Full Product Set (FPS) of the GlobColour Archive (http://hermes.acri.fr/) version

1. Results of the regional and global validation of the Chl-*a* product have been published in Maritorena et al. (2010) where the merged GlobColour data were validated through matchup analyses and by comparing them to the validation results of Chl-*a* data sets obtained from individual missions. GlobColour data showed the same high similar quality as the standard SeaWiFS empirical Chl-*a* algorithm OC4v4 (Maritorena et al. 2010). The uncertainty for the GlobColour product is provided on a pixel–pixel basis and is for the Southern Ocean region mostly far below 20 %, but can reach in certain cases (close to sea-ice) up to 40 %. Mean and standard deviation values of satellite Chl-*a* concentration (mg Chl-*a* m^{-3}) and sea-ice concentration (in %) were extracted for each OFOS station. As collocation criterion, satellite data were selected, measured exactly at the station location and within the 3 × 3 pixel box of the direct satellite collocation. Satellite data within three different time frames were selected. These existed for the 10 years prior to the cruise (2003–2012), the 5 years prior the cruise (2008–2012) and the last 30 days together with the actual day when the sampling took place. For the 31-day means, daily data were used, and monthly outputs were used for the 10-year and 5-year mean results. For measurements of

Table 1 Station data for locations where seabed photographs were obtained along 2-km-long transects during cruise ANT-XXIX/3 of RV *Polarstern* to the waters off the northern Antarctic Peninsula in January–March 2013

Station no.	Station label	Depth (m)	Temperature (°C)	Salinity	Chl-*a* 5 years (mg m^{-3})	Sea ice 5 years (%)
160-1	WS-JE-B	233	−1.75	34.49	0.38 ± 0.55	44.11 ± 90.84
161-1	WS-ET-B	238	−1.87	34.54	0.74 ± 1.40	50.11 ± 91.10
163-2	WS-ET-D	481	−1.77	34.43	1.35 ± 2.04	54.08 ± 97.08
164-2	WS-DV-B	148	−1.34	34.46	0.63 ± 0.87	62.58 ± 82.25
NG-B	WS-NG-B	191	−1.76	34.51	0.96 ± 1.15	57.79 ± 95.40
NG-U	WS-NG-U	214	−1.60	34.38	0.96 ± 1.15	57.79 ± 95.40
NG-S	WS-NG-S	380	−1.60	34.33	0.95 ± 1.14	57.79 ± 95.40
NG-D	WS-NG-D	78	−1.46	34.47	0.96 ± 1.14	57.64 ± 95.29
116-3	BS-JN-B	215	−1.54	34.47	0.24 ± 0.13	32.81 ± 92.62
118-3	BS-JN-U	426	−1.15	34.52	0.28 ± 0.16	32.34 ± 92.75
194-1	BS-E-B	177	−1.56	34.54	0.24 ± 0.17	29.97 ± 86.65
197-3	BS-E-U	194	−1.47	34.43	0.27 ± 0.17	28.96 ± 87.36
192-1	BS-E-S	434	−0.96	34.50	0.29 ± 0.18	28.98 ± 87.85
196-2	BS-E-D	479	−1.31	34.47	0.23 ± 0.14	28.78 ± 84.04
198-2	BS-C-B	175	−1.29	34.41	0.22 ± 0.10	28.34 ± 87.04
199-1	BS-C-U	302	−1.33	34.48	0.25 ± 0.11	28.47 ± 88.79
215-2	BS-C-S	449	−0.95	34.56	0.34 ± 0.18	28.35 ± 88.86
204-1	BS-C-D	765	−0.72	34.54	0.26 ± 0.13	28.42 ± 87.21
222-2a	BS-W-B	160	−1.21	34.56	0.32 ± 0.29	28.05 ± 89.08
222-2b	BS-W-U	268	−1.20	34.41	0.30 ± 0.23	28.10 ± 89.27
225-6	BS-W-S	553	−0.85	34.47	0.35 ± 0.24	27.07 ± 88.15
218-3	BS-W-D	746	−0.80	34.55	0.24 ± 0.17	28.16 ± 89.09
246-1	DP-E-U	281	−0.16	34.42	0.47 ± 0.36	7.29 ± 48.98
249-1	DP-E-S	414	0.12	34.51	0.51 ± 0.45	7.24 ± 49.11
251-1	DP-C-U	274	0.04	34.55	0.48 ± 0.42	7.58 ± 50.39
244-1	DP-C-S	419	0.62	34.44	0.48 ± 0.44	7.58 ± 50.39
234-3	DP-W-U	239	0.03	34.53	0.47 ± 0.38	7.55 ± 49.84
237-2	DP-W-S	385	0.42	34.40	0.46 ± 0.39	7.51 ± 49.73

Stations are categorized according to study region: Weddell Sea (WS), Bransfield Strait (BS) and Drake Passage (DP); regional habitat blocks and habitats (*B* bank, *U* upper slope, *S* slope, *D* deep/canyon). Transects at Nachtigaller Shoal (stations 185, 186, 188, 189) spanned a wide depth range and were consequently divided into habitat-specific sections. Average water depths, water column properties (bottom-water temperature and salinity). See Online Resource 1 for more station data

Chl-*a*, the standard deviation considering only January and February values of the 10 as well the 5 span of years was present.

Seabed morphology along the OFOS tracks was obtained from the analysis of bathymetric data recorded with an Atlas Hydrosweep DS3 deepwater multibeam echosounder with a vertical accuracy better than 0.2 % of the water depth. The data were post-processed with the hydrographic software package Caris Hips and Sips® 8.0 to remove artifacts related to erroneous calibration values and spurious soundings and for sound velocity corrections (for further details, see Dorschel et al. 2015). From the clean multibeam echosounder data, digital terrain models (DTM) were calculated with 30-m grid cell size for each survey region. The DTMs were projected to UTM Zone 21S with a datum of WGS 1984 and form the basis for all subsequent geostatistical analyses performed with ESRI software package ArcGIS® including the toolbox extensions Benthic Terrain Modeler (BTM) (Wright et al. 2005). For this study, the ruggedness and the slope inclination of the terrain were calculated. Ruggedness was calculated with the BTM toolbox extension (Wright et al. 2005) as measure for the rugosity or 'bumpiness' of the seabed (Wilson et al. 2007), while the slope or inclination of the terrain (the first derivative of the topography) was calculated in ArcGIS® following the approach of Burrough and McDonell (1998). With the BTM, based on the bathymetric position index (Weiss 2001), the following

terrain classes were used: (1) Flat Plains, (2) Broad Slopes, (3) Steep Slopes, (4) Current Scoured Depressions, (5) Scarp/Cliff, (6) Depression, (7) Crevices, Narrow Gullies over elevated terrain, (8) Flat Ridge Tops, (9) Rock Outcrop High, Narrow Ridge, (10) Local Ridge, Boulders, Pinnacles in Depression, (11) Local Ridge, Boulders, Pinnacles on Broad Flats, (12) Local Ridge, Boulders, Pinnacles on Slopes, (13) Local Depression, Current Scours, (14) Plateau. The classification followed an approach proposed by Wright et al. (2005), which was modified after Wienberg et al. (2013) and Dorschel et al. (2014). One terrain class was designated to each seabed photograph, and the frequencies of the terrain classes across the 100 photographs of each transect were computed (Table 2).

Data analysis

Faunistic resemblances among transects were quantified using pairwise Bray–Curtis similarities (Bray and Curtis 1957) computed based on square-root-transformed ascidian abundance values. In the analysis, single photographs were treated as replicates at transect level.

A permutational multivariate analysis of variance (PERMANOVA; Anderson 2001) was performed to analyze differences in ascidian composition across spatial scales using a mixed hierarchical design with three factors ('Region' = fixed with three levels, 'Depth Zone' = fixed with two levels and fully crossed with 'Region,' and 'Station' = random and nested within 'Region × Depth Zone') based on the Bray–Curtis similarity matrix. The

Table 2 Abundances of terrain classes for each station summarized by single counts of terrain classes for each photograph of the transect

Station no.	Station label	1	2	3	4	5	6	7	8	9	10	11	12	13	14
160-1	WS-JE-B	100	0	0	0	0	0	0	0	0	0	0	0	0	0
161-1	WS-ET-B	100	0	0	0	0	0	0	0	0	0	0	0	0	0
163-2	WS-ET-D	100	0	0	0	0	0	0	0	0	0	0	0	0	0
164-2	WS-DV-B	98	2	0	0	0	0	0	0	0	0	0	0	0	0
NG-B	WS-NG-B	0	0	0	0	0	0	0	100	0	0	0	0	0	0
NG-U	WS-NG-U	8	6	2	0	3	0	2	64	11	0	0	4	0	0
NG-S	WS-NG-S	56	28	11	0	0	0	0	0	0	0	0	3	2	0
NG-D	WS-NG-D	97	0	0	0	1	0	0	0	0	0	0	2	0	0
116-3	BS-JN-B	95	0	1	0	0	0	0	0	0	0	1	2	1	0
118-3	BS-JN-U	98	2	0	0	0	0	0	0	0	0	0	0	0	0
194-1	BS-E-B	100	0	0	0	0	0	0	0	0	0	0	0	0	0
197-3	BS-E-U	82	15	0	0	0	0	0	0	0	0	0	1	2	0
192-1	BS-E-S	100	0	0	0	0	0	0	0	0	0	0	0	0	0
196-2	BS-E-D	6	16	0	67	0	4	0	0	0	5	0	2	0	0
198-2	BS-C-B	90	10	0	0	0	0	0	0	0	0	0	0	0	0
199-1	BS-C-U	100	0	0	0	0	0	0	0	0	0	0	0	0	0
215-2	BS-C-S	67	33	0	0	0	0	0	0	0	0	0	0	0	0
204-1	BS-C-D	99	1	0	0	0	0	0	0	0	0	0	0	0	0
222-2a	BS-W-B	100	0	0	0	0	0	0	0	0	0	0	0	0	0
222-2b	BS-W-U	100	0	0	0	0	0	0	0	0	0	0	0	0	0
225-6	BS-W-S	97	3	0	0	0	0	0	0	0	0	0	0	0	0
218-3	BS-W-D	99	1	0	0	0	0	0	0	0	0	0	0	0	0
246-1	DP-E-U	94	6	0	0	0	0	0	0	0	0	0	0	0	0
249-1	DP-E-S	78	22	0	0	0	0	0	0	0	0	0	0	0	0
251-1	DP-C-U	0	0	0	0	0	0	0	100	0	0	0	0	0	0
244-1	DP-C-S	0	46	52	0	1	0	0	0	0	0	0	1	0	0
234-3	DP-W-U	89	0	0	0	0	0	0	11	0	0	0	0	0	0
237-2	DP-W-S	0	6	53	12	3	2	3	16	5	0	0	0	0	0

The following terrains classes were used for the analysis: (1) Flat Plains, (2) Broad Slopes, (3) Steep Slopes, (4) Current Scoured Depressions, (5) Scarp/Cliff, (6) Depression, (7) Crevices, Narrow Gullies over elevated terrain, (8) Flat Ridge Tops, (9) Rock Outcrop High, Narrow Ridge, (10) Local Ridge, Boulders, Pinnacles in Depression, (11) Local Ridge, Boulders, Pinnacles on Broad Flats, (12) Local Ridge, Boulders, Pinnacles on Slopes, (13) Local Depression, Current Scours, (14) Plateau. Transects at the Nachtigaller Shoal (stations 185, 186, 188, 189) spanned a wide depth range and were consequently divided into habitat-specific sections

analysis was run using the permutation of residuals under a reduced model with 999 permutations and type III sums of squares. PERMANOVA pairwise tests were conducted for significant sources of variation between the factors. Subsequently, a PERMDISP analysis was performed on the same Bray–Curtis similarity matrix to determine the nature of the difference (location, spread, or a combination of the two) between any pair of groups.

Indicator species of the three regions were determined with the similarity percentage procedure (SIMPER; Clarke and Warwick 1994), based on the within- and between-station differences in community composition. This analysis allows identifying the taxa and systematic/morphological bulk groups that contribute to the observed similarity or dissimilarity between samples. The higher the abundance of a given taxon or bulk group within a station group, the more it contributes to the pattern (Clarke 1993).

To further analyze differences between habitats at the intermediate (10-km), mainly depth-related spatial scale including all four habitat types (B, U, S, D), we used one-way ANOSIM (ANalysis Of SIMilarity; Clarke 1993) for the two regions where all habitats were sampled (WS, BS), based on the Bray-Curtis similarity matrix calculated from the photographic replicates.

Non-metric multidimensional scaling (nMDS) was used to display among-transect resemblance patterns in ascidian composition in a two-dimensional plot (Kruskal and Wish 1978). A low nMDS stress coefficient indicates that the multivariate resemblance pattern is represented by the distances between the stations in the plot without much distortion (Clarke 1993).

Distance-based analysis on a linear model (DistLM) was carried out to assess the relative contributions of environmental variables in structuring ascidian assemblages at the large spatial scale (Anderson et al. 2008). The set of the stationwise frequencies of the 14 terrain classes (Table 2) was assigned to an 'indicator' in the DistLM. Prior to the actual analysis, the full set of all available environmental variables was tested for redundancy with the Draftsman's plot. Variables with a correlation of $r > 0.85$ were omitted from the model (Online Resource 2). Environmental data were normalized, and Bray–Curtis similarity between all replicates based on ascidian abundance was calculated. The DistLM routine was based on Akaike's information criterion (AICc), corrected to account for small sample size compared with the number of predictor variables (Burnham and Anderson 2004). AIC describes the quality of the model, with small values indicating higher quality. As selection criterion, the 'Best' procedure was used. Additionally, the analysis was performed with the selection criterion 'Adjusted R^2,' which takes the total number of variables into account, but also changes relative to the complexity of the system. Through the combination of both

selection criteria the optimal model for a combination of variables that can best explain the pattern of ascidian assemblages was determined. DistLM analysis tests the general null hypothesis of no relationship. The pattern was visualized with a 'distance-based redundancy analysis' (dbRDA) plot, which is generally used to perform an ordination of fitted values from a given model. In a dbRDA plot, the first two axes are shown, which represent the highest percentage of explained variation of the fitted model and the total variation.

All statistical analyses were performed using PRIMER software version 6.1.6 (Clarke and Gorley 2006).

Results

Environmental setting

Bottom-water temperatures (Table 1) ranged in the Drake Passage from −0.16 to 0.62 °C. In the Bransfield Strait, temperatures were lower (−1.56 to −0.72 °C). The Weddell Sea had the coldest bottom water with −1.87 to −1.34 °C (for details, see Hunke et al. in review). Bottom-water salinity ranged between 34.33 and 34.56 and was lowest in the Weddell Sea (Table 1).

Satellite data showed highest surface Chl-a concentrations in the Weddell Sea and lowest in the Bransfield Strait (Table 1). Average sea-ice cover in the 5-year period before sampling in 2013 was highest in the Weddell Sea (approximately 60 %) and lowest in the Drake Passage (approximately 8 %) (Table 1).

The Benthic Terrain Modeler detected the class 'Flat Plains' for the majority of the photographs at all stations. At stations WS_NG_B, WS_NG_U, and DP_C_U, mostly 'Flat Ridge Tops' were present in the photographs, and at stations DP_C_S and DP_E_S, 'Slope Stations' were commonly found. Station BS_C_B was dominated by the category 'Depression' and station BS_E_D by 'Current Scoured' (Table 2). In none of the photographs at any of the stations, iceberg scours were visible.

Composition and abundance

A total of 45,363 individuals were counted on 2800 seabed photographs analyzed from 28 stations. In the photographs, five ascidian species were identified: *Pyura bouvetensis* (Michaelsen, 1904) (Fig. 2a), *Distaplia cylindrica* (Lesson, 1830) (Fig. 2b), *Aplidium radiatum* (Sluiter, 1906) (Fig. 2c), *Cnemidocarpa verrucosa* (Lesson, 1830) (Fig. 2d) and *Molgula pedunculata* (Herdmann, 1881) (Fig. 2e). Three species could not be identified conclusively in the photographs (Fig. 2f–h) and were thus allocated to the putative species *Synoicum* sp. (Fig. 2f), compound Ascidiacea sp. 1
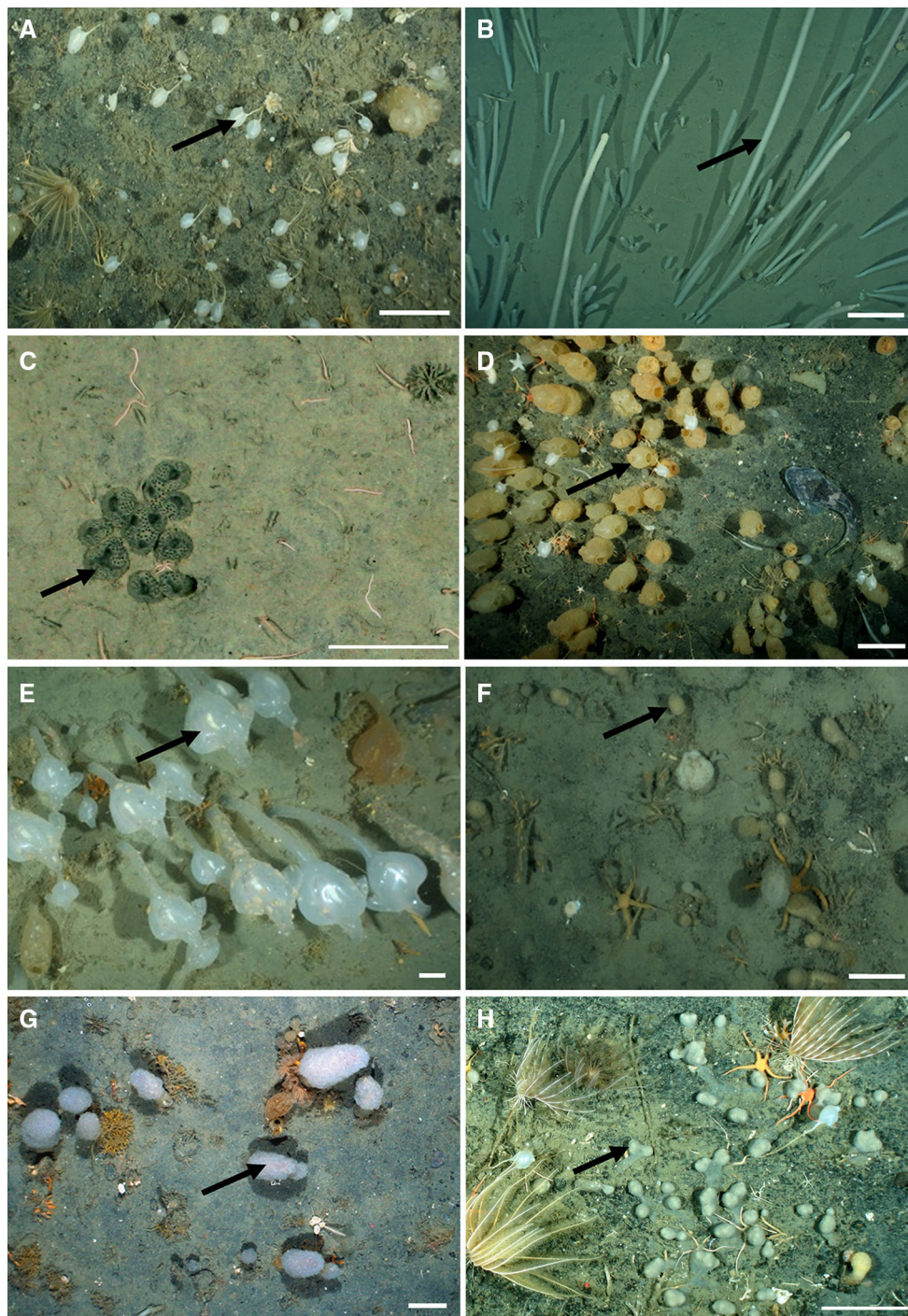
Fig. 2 Seabed photographs showing examples of the most common ascidian taxa off the northern Antarctic Peninsula in January–March 2013: **a** *Pyura bouvetensis*; **b** *Distaplia cylindrica*; **c** *Aplidium radiatum;* **d** *Cnemidocarpa verrucosa*; **e** *Molgula pedunculata*; **f** *Synoicum* sp.; **g** compound Ascidiacea sp. 1; **h** compound Ascidiacea sp. 2. *Scale bars* at each photograph represent approximately 10 cm

(Fig. 2g) and compound Ascidiacea sp. 2 (Fig. 2h). Ascidian specimens that could not be identified to species level were classified as solitary Ascidiacea indeterminata (indet.) or as compound Ascidiacea indet. Overall, most abundant were the compound Ascidiacea *D. cylindrica* with 7914

specimens and *P. bouvetensis* with 7121 specimens (Online Resource 3). Composition and abundance of the ascidian assemblages differed pronouncedly among the study regions (Fig. 3). Overall, both abundance and taxonomic richness were lower at Drake Passage stations than in the other two

regions. *D. cylindrica* commonly dominated the assemblages at the Weddell Sea stations, while compound Ascidiacea sp. 2 reached its highest abundances in the Bransfield Strait. Ascidian abundance was highest in Bransfield Strait at station BS-JN-B (Fig. 3), with a total of 13,625 specimens (36.61 ± 11.35 ind. m^{-2}), while fewest specimens were detected in Bransfield Strait at station BS-C-D (0.2 ± 0.15 ind. m^{-2}) and in Drake Passage at stations DP-E-S (0.25 ± 0.14 ind. m^{-2}) and DP-E-U (0.35 ± 0.17 ind. m^{-2}).

Spatial distribution

PERMANOVA revealed significant differences in ascidian assemblages at two spatial scales: between 'Region' and between 'Station' (Table 3). In contrast, no significant differences were present with regard to the intermediate-scale factor 'Depth' and the interaction term 'Region × Depth' (Table 3). Pairwise between-region PERMANOVA comparisons revealed that the Weddell Sea was significantly different from the other two regions (BS × WS: $p = 0.003$; WS × DP: $p = 0.001$), while no significant differences were detected between Drake Passage and Bransfield Strait ($p = 0.076$). However,

Table 3 Results of PERMANOVA for the test of the significance of differences in ascidian assemblages among the three regions off the Antarctic Peninsula and between the two-category factor 'Depth'

Source	df	Pseudo-F	p (perm)
Region	2	5.5734	0.001*
Depth	1	2.2935	0.09
Region × depth	2	0.7662	0.591
Station (region × depth)	22	90.939	0.001*
Residuals	2772		
Total	2799		

df degrees of freedom, *p* (*perm*) significance level assessed from permutation test

* Significant results [*p* (*perm*) > 0.05]

PERMDISP analyses revealed that caution should be taken in the interpretation of the PERMANOVA results because they indicated that between-region differences can also be due to differences in their within-region variation ('Region': $F = 148.27$; $p = 0.001$; 'Depth': $F = 971.43$; $p = 0.001$).

One-way ANOSIM tests showed no significant within-region differences in the composition of the ascidian assemblages among the intermediate-scale benthic habitats
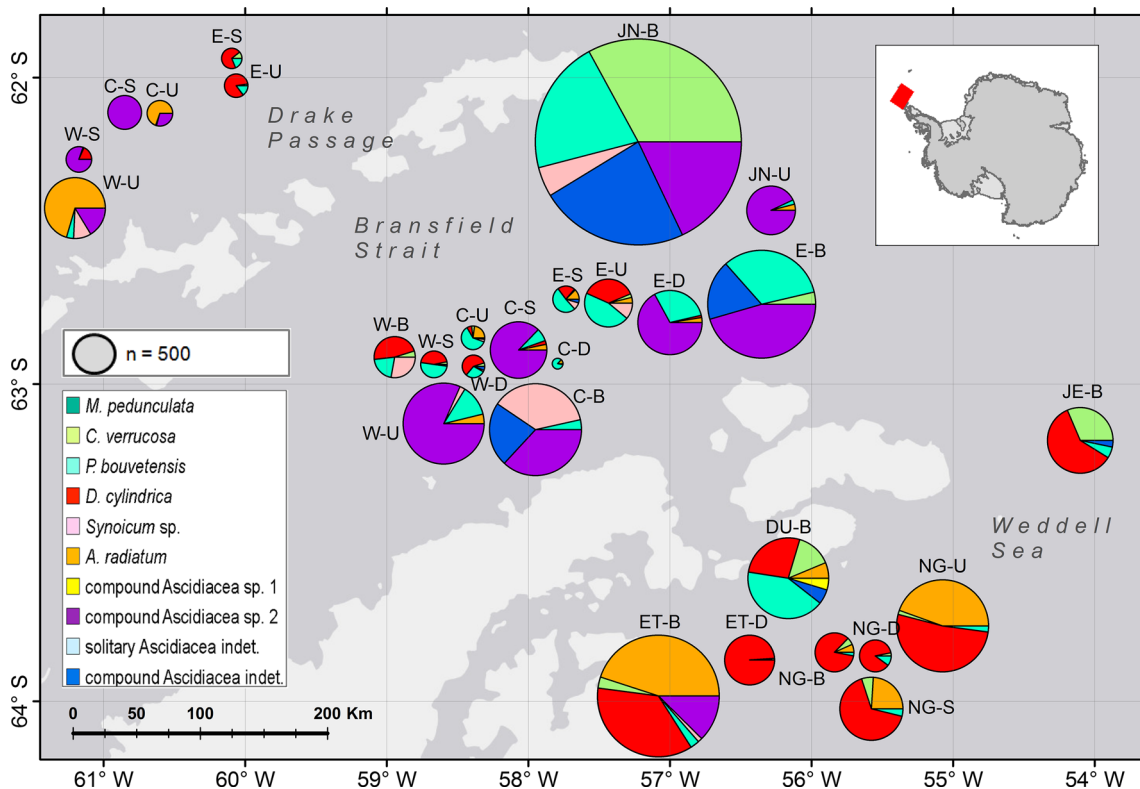

Fig. 3 Regional distribution, composition and abundance of ascidian assemblages off the northern Antarctic Peninsula in January–March 2013. The size of the *pie charts* represents the total abundance of the ascidian fauna at each station (for station labels see Table 1); the pie sectors display the abundance proportions of ascidian taxa at each station. (Color figure online)

bank, upper slope, slope and deep/canyon in the Weddell Sea ($R = -0.020$; $p = 0.536$) and the Bransfield Strait ($R = 0.072$; $p = 0.271$).

The nMDS plot illustrates the PERMANOVA results, with a grouping of Weddell Sea stations in the upper part of the plot, while there is no clear separation between the stations of the Drake Passage and those of the Bransfield Strait, and neither among benthic habitats (Fig. 4a). Moreover, overlays of the abundance of selected ascidian species illustrate that *D. cylindrica* is largely confined to Weddell Sea stations (Fig. 4b), corroborating the results of the SIMPER analysis (Table 4), while compound Ascidiacea indet. were almost exclusively found at stations of the lower cluster in the plot (Fig. 4c).

SIMPER analyses showed that *D. cylindrica* contributed about 91 % to the total Bray–Curtis similarity of about 31 % among Weddell Sea stations, as well as 37 and 46 %, respectively, to the between-region dissimilarity of the Weddell Sea to the Bransfield Strait and Drake Passage, respectively (Table 4). Overall, the within-region Bray–Curtis similarity of the other two regions was clearly lower (20 and 15 %) than that of the Weddell Sea (Table 4). *P. bouvetensis* contributed most (49 %) to the total Bray–Curtis similarity between Bransfield Strait stations, while compound Ascidiacea indet. did so (with about 56 %) for the Drake Passage stations.

At the small-scale (within-transect, i.e., 2-km) level, the ascidian abundances varied markedly (see Fig. 5 for four examples). At station DP-W-S in the Drake Passage, diversity was low and abundances differed considerably among photographs at a relatively low spatial scale (Fig. 5a). In comparison, station BS-JN-B was characterized by a high within-photo diversity, high abundances and an obviously changing composition along the 2-km transect (Fig. 5b). For example, *C. verrucosa* occurred only in the second half of the transect. At the deep station BS-C-D in the Bransfield Strait, no ascidians were present in many photographs, while in the remainder almost only *P. bouvetensis* occurred, albeit at very low abundances (Fig. 5c). At station WS-ET-B in the Weddell Sea, several ascidian taxa were counted on most photographs, with *D. cylindrica* and *P. bouvetensis* being the most abundant species (Fig. 5d). Compound Ascidiacea sp. 2 only occurred on two consecutive photographs. For small-scale distribution patterns along other transects, see further plots in Online Resource 4.

Correlation between environmental and biotic patterns

DistLM analysis showed that a combination of bottom-water oxygen, bottom-water salinity, sea-ice cover (5-year averages) and bottom rugosity explained about 30 % of the between-station variation in ascidian abundances (AIC value of 174.69; adjusted R^2 value of 0.187; Table 5).

The two axes of the distance-based redundancy analyses (dbRDA) plot (Fig. 6) explained 29.5 and 1.2 %, respectively, of the total variation in the ascidian abundance data. The position of the environmental vectors in the plot suggests that most of the variation along Axis 1 is explained by the gradient in sea-ice cover.

Discussion

This investigation was designed to increase our knowledge on the occurrence and distribution of shelf-inhabiting ascidians in an ecologically complex region of the Southern Ocean at large, intermediate and small spatial scales. The three selected regions differed markedly in their large-scale physical properties, while intermediate-scale habitats were hypothesized to be characterized by different current regimes, sediment compositions and food supply. Together with the small-scale distribution patterns of the organisms and information on the bottom topography documented along photographic transect, three hypotheses were tested.

Regional patterns

Our investigation provided clear evidence of significant differences in the composition and abundance of ascidian assemblages on a regional scale off the northern Antarctic Peninsula, confirming our hypothesis 1a): At a large scale (100 km), ascidian assemblages differed significantly among regions. This pattern is probably associated with the spatial distribution of water masses in this region. The northwestern Weddell Sea is characterized by distinctly colder waters than the regions off the western side of the peninsula (Cape et al. 2014). This is primarily caused by cold surface-water masses, which are transported northward along the eastern side of the Antarctic Peninsula as part of the clockwise Weddell Gyre. The Bransfield Strait west of the northern Antarctic Peninsula is slightly warmer, caused by a flooding of the shelf by the Circumpolar Deep Water from the Antarctic Circumpolar Current that mixes at the tip of the Antarctic Peninsula with the colder Weddell Gyre water (Orsi et al. 1995; Clarke et al. 2009). This pronounced hydrographic difference is clearly correlated with the regional distribution of the ascidian assemblages in these three study regions. A similar relationship was also found for the distribution of megafaunal assemblages off the South Shetland Islands and the northern Antarctic Peninsula (Lockhart and Jones 2008).

Satellite observations for the period January–March 2013 showed that the Weddell Sea was mostly covered

Fig. 4 MDS plots displaying the between-station Bray–Curtis resemblance pattern of the ascidian fauna, computed from square-root-transformed abundance data of replicate photographs. **a** *Symbols* represent the three different regions Weddell Sea (*WS*), Bransfield Strait (*BS*) and Drake Passage (*DP*) and merged habitats for the factor 'Depth,' while letters denote the benthic habitats bank (*B*), upper slope (*U*), slope (*S*) and deep/canyon (*D*) within each region. Circle sizes represent the average abundance of *D. cylindrica* (**b**) and compound Ascidiacea indet. **c** at each station
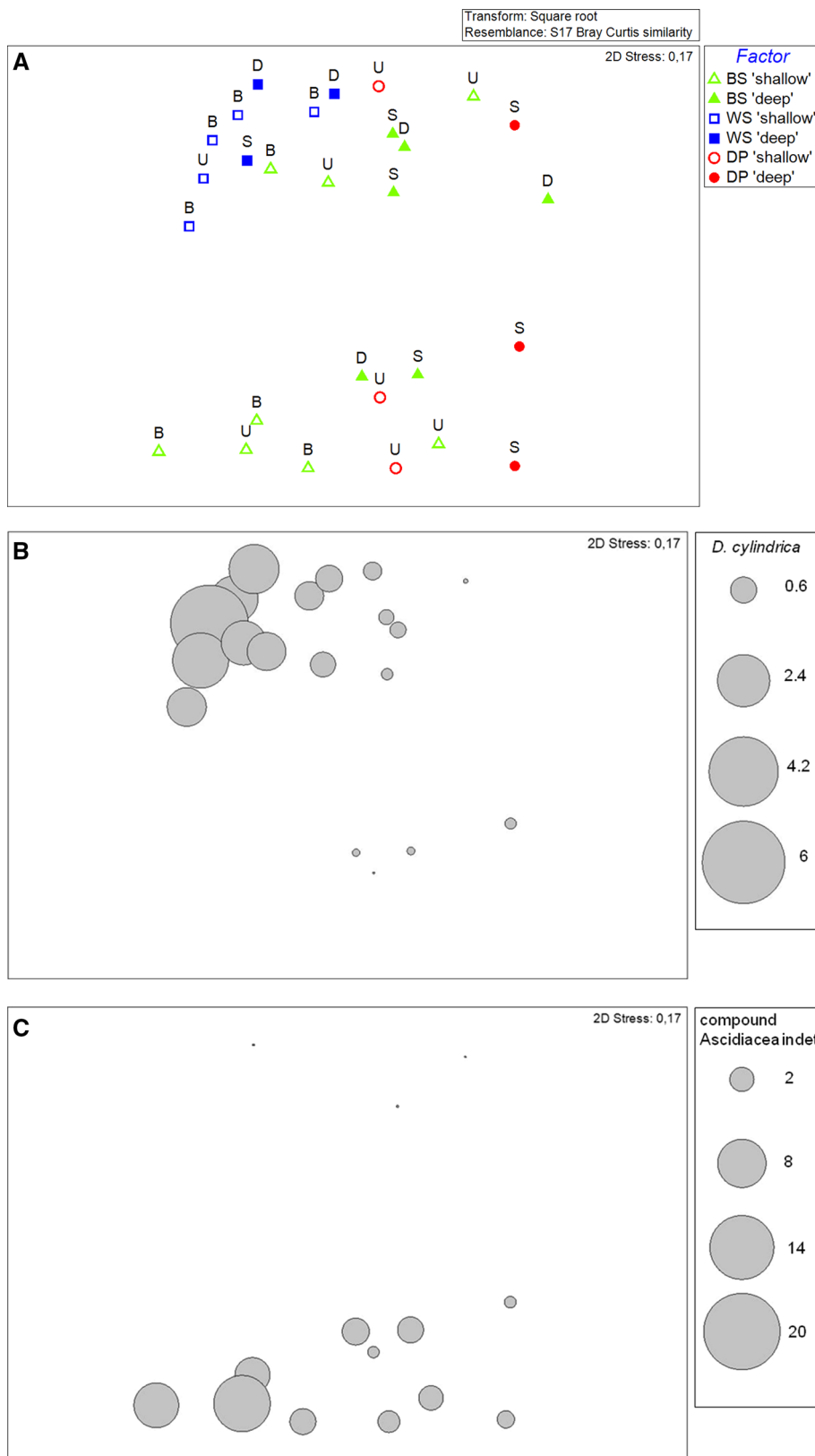
with sea ice, whereas the Drake Passage with its nearly oceanic conditions was almost ice free. We found evidence, suggesting that the sea-ice cover during the last 5

years (together with salinity, oxygen and bottom rugosity) had an influence on the distribution of ascidians, corroborating our hypothesis (1b): Variation in major

Table 4 Results of regional-scale (between-region) SIMPER analysis

Typifying species	Weddell Sea	Bransfield Strait	Drake Passage
(a)			
A. radiatum	–	–	23.7
D. cylindrica	90.9	6.0	17.7
P. bouvetensis	–	48.6	–
Compound Ascidiacea indet.	–	39.6	55.8
Within-region similarity	30.6	19.8	15.4

Discriminating species	Weddell Sea vs. Bransfield Strait	Weddell Sea vs. Drake Passage	Bransfield Strait vs. Drake Passage
(b)			
A. radiatum	–	16.6	–
C. verrucosa	7.6	–	–
D. cylindrica	37.1	45.6	6.2
P. bouvetensis	21.3	9.9	15.5
Compound Ascidiacea indet.	20.5	19.0	33.4
Synoicum sp.	4.9	–	–
Between-region dissimilarity	90.6	91.6	88.3

Contributions (%) of (a) typifying and (b) discriminating ascidian species to (a) within-region Bray–Curtis similarities (%) and (b) between-region Bray–Curtis dissimilarities (%)

environmental parameters, such as water masses and sea-ice coverage, which effect primary production providing food for the benthos, can explain these differences in ascidian distribution with only 30 %. It is clear, however, that sea ice does not have a direct effect on the ascidians but can rather be considered as a proxy for availability of food. Sea ice is crucial for a variety of physical and biological processes, as it can both reduce and enhance the productivity of the euphotic zone and, therefore, the strength of the pelagic–benthic coupling through flux of particles to the sea floor (Clarke and Ackley 1984; Fischer et al. 1988). The dynamics of polar marine ecosystems are dominated by the seasonal growth, extent and retreat of sea ice and their interannual variations (Ducklow et al. 2006). Below the euphotic zone, photosynthesis is not possible and thus the benthos depends on the vertical and horizontal influx of food (Tatián et al. 2005).

We recorded more ascidians in the almost year-round ice-covered Weddell Sea and seasonally ice-covered Bransfield Strait than in the almost ice-free Drake Passage. Sea ice is an explanatory factor for the distribution of ascidians since it could be a proxy for the different water masses. In the austral summer, regional high phytoplankton blooms caused by a melting of the sea-ice are possible which can increase the annual primary production (Lizotte 2001; Arrigo and Thomas 2004). Therefore, in the Marginal Ice Zone the production is higher than in permanently open waters like the Drake Passage (Lizotte 2001).

The factor assumed to be most directly related to food supply—Chl-a concentrations in surface waters—did not

have a strong effect on the ascidian assemblages in this investigation. Two possible explanations for the strong link between 5-year sea-ice cover and ascidian assemblages can be provided: (1) Sea ice is rather a proxy for general oceanographic and climatic characteristics than for the general productivity of the different regions and the food supply to the benthos (Smith et al. 2006) or (2) intense diatom blooms in areas with high sea-ice cover with leaks and below the sea-ice, that cannot be measured through the satellite-derived surface Chl-a used in our study, have provided sufficient or more food input to benthic communities in the Weddell Sea and Bransfield Strait.

Intermediate-scale gradients

Generally, one can assume that differences in bottom topography at the 10-km scale strongly affect current conditions and, as a consequence, also sediment composition. The factor 'Depth' was chosen in this study as a proxy of topographic habitat regimes. It was hypothesized that on shelf plateaus and close to their margins at the upper slope the bottom-current velocity was higher and resulted in coarser sediments due to the winnowing effect. Since suspension feeders like ascidians can only exist if sufficient quantities of food particles drift through the water above the seabed (Kowalke 1999), they can be expected to be especially abundant in regions characterized by high average current velocities. In depressions with low current velocity, organic particles sink relatively fast to the sea-floor where they are deposited and are therefore easily
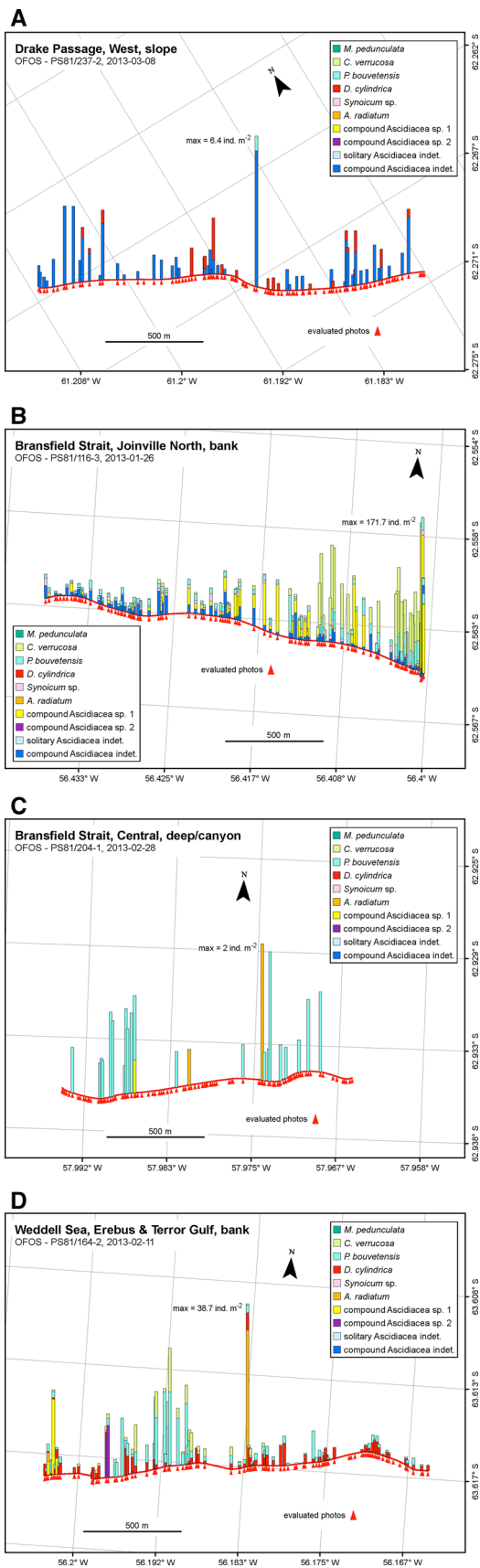
Fig. 5 Detailed maps showing the position of seabed photographs taken along four selected 2-km transects off the northern Antarctic Peninsula in January–March 2013 and the abundance of ascidian species (ind m^{-2}) in stacked bar charts for each single photograph randomly selected for evaluation: **a** DP-W-S; **b** BS-JN-B; **c** BS-C-D; **d** WS-ET-B. See Online Resource 4 for more transects. (Color figure online)

Table 5 Results of the 'distance-based analysis on a linear model' (DistLM) used to identify the combination of environmental factors (1 = salinity; 2 = oxygen; 3 = sea-ice cover (5-year averages); 4 = terrain classes (BTM) index; 5 = bottom rugosity (mean); 6 = bottom rugosity (standard deviation); 7 = water depth) with the highest correlation to the ascidian distribution pattern

Factor selections	AICc	Adj R^2	R^2	No. of groups
1;2;3;4	208.26	0.18993	0.57996	4
1;2;3;5	174.69	0.18684	0.30731	4
1;2;3;6	175.16	0.17302	0.29553	4
1;2;3;5;7	177.29	0.16995	0.32367	5
1;2;3	173.58	0.16641	0.25903	3

Selection is based on the values of Akaike's information criterion (AICc) and adjusted R^2 of the models

accessible for deposit feeders, as suspension feeders are not able to use particles directly from the sediment surface (Gutt and Starmans 1998; Kowalke 1999).

However, no significant difference was detected between the habitats nor with regard to the factor 'Depth' in our data and we cannot corroborate our hypothesis (2): At an intermediate scale (10 km), habitats within each of the large regions are different. The seabed photographs clearly indicated that at most stations, even at the shallower and assumed more dynamic sites, the seabed was dominated by fine sediments. Particularly the Drake Passage stations were characterized by very fine mud-like substrate. Only in the Bransfield Strait and Weddell Sea, patches of coarser sediments and stones occurred, which are the preferred settling substrates for ascidians (Young and Chia 1984). Consequently, ascidian abundances were generally higher in these regions. The Benthic Terrain Modeler distinguished different terrain classes in our bottom topography data, with 'Flat Plains' as the most common category. The seabed ruggedness, correlated with the slope angle of the terrain, had an influence on the distribution of ascidians at a small scale. Tatián et al. (1998b) reported that *Cnemidocarpa verrucosa* and *Pyura bouvetensis* occur on fine sediments, as well as on hard substrata, which could be an explanation for the generally high abundances of these species in this study. These three species, as well as *Distaplia cylindrica*, the most abundant species in our study, are able to form either expanded holdfasts or rootlets

Fig. 6 dbRDA-plot based on the result from the DistLM analysis for the variables that best explain the species distributions
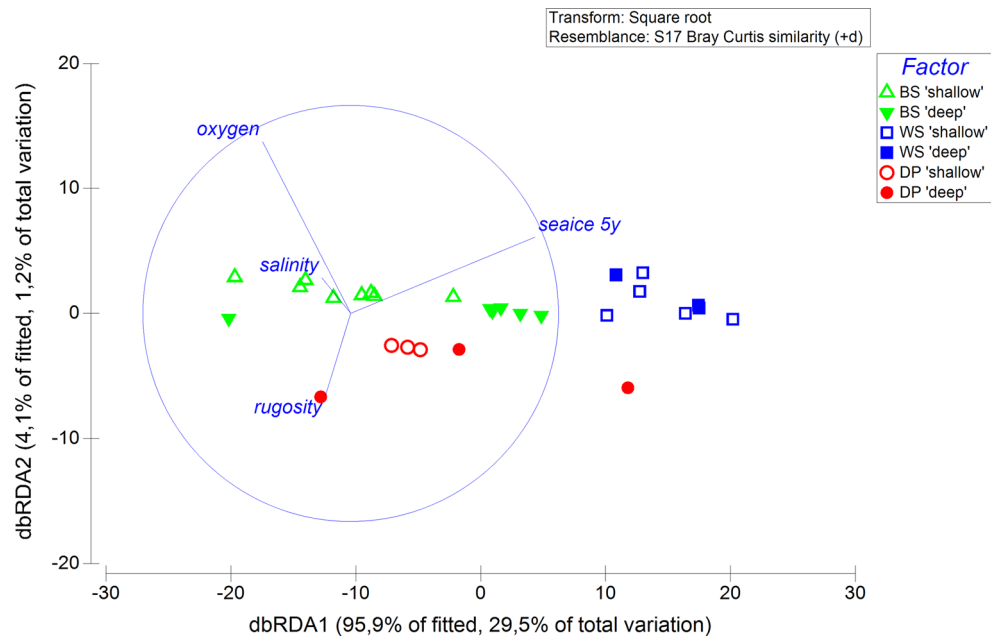
that allow them to settle on fine sediments (Tatián et al. 1998b). However, fine sediments are often resuspended by bottom currents or other species, and a constantly strong silting can have a negative influence on sessile organisms, such as ascidians, since it causes burial and clogging of the siphons and the brachial wall (Bakus 1968). Stalked ascidians like *P. bouvetensis* and *D. cylindrica* obviously benefit from their morphology by the heightened position of their feeding apparatuses above the sediment. Therefore, they can exist in regions with sediment turbulence and may improve food capture during periods of low primary production (Gili et al. 2001).

Although the ascidian fauna off the Antarctic Peninsula and in Weddell Sea are composed by more than 70 species (Primo and Vázquez 2009), the stations under investigation were largely dominated by only a few species, *D. cylindrica* in the Weddell Sea and *P. bouvetensis* in the Bransfield Strait. This pronounced dominance may have masked finer faunistic between-habitat differences. The general occurrence of most of the species, taxa or bulk groups in these three environmentally quite different regions may be explained by their plasticity allowing them to cope with various environmental conditions. Their lack at single stations, however, must be explained by other unknown inhibiting factors operating at the intermediate spatial scale.

Small-scale dispersion

The small-scale environmental heterogeneity plays an important role in structuring the ascidian assemblages in our study, as indicated by the pronounced patchiness in the

distribution of ascidians within the 2-km transects. Sessile organisms such as ascidians, but also sponges, cnidarians and mobile organisms, can reach high densities in local patches, which have been described as being typical of the Antarctic (Gutt and Piepenburg 1991; Gutt and Koltun 1995; Gutt and Starmans 1998; Sahade et al. 1998). These can be caused by spatial variability at the 1–10-m scale in seabed properties (Tatián et al. 1998a) and water-mass characteristics, which results in pronounced differences in food availability In addition, such patterns can be shaped by biological processes such as reproduction, larval dispersal (Woodin 1976, 1978), recruitment success, population growth, mortality (Gutt et al. 2013), behavior (Gutt and Piepenburg 1991), as well as competition and predation (Jackson and Buss 1975; Jackson 1977; Young and Chia 1984).The early life history of ascidians in particular should be taken into consideration. In general, ascidians propagate by planktonic non-feeding larvae that develop rapidly and settle early (Svane and Young 1989; Strathmann et al. 2006). Dispersal, settlement and metamorphosis must be achieved within the brief larval phase. The scale at which active selection of substratum occurs is additionally determined by hydrodynamic conditions (Butman 1987). In general, recruitment and settlement are strongly affected by the interplay between larval mobility and behavior, duration of the larval phase (Svane and Havenhand 1993; Petersen and Svane 1995), current patterns (Davis and Butler 1989; Smith and Witman 1999), physicochemical properties of benthic habitats (Davis 1987; Keough 1998), as well as the presence of already settled ascidians (Osman and Whitlatch 1995; Keough 1998; Rius et al. 2010). Grave (1936) showed that chemical

cues influence the timing of larval establishment. Larvae metamorphose faster when the water column is mixed with extracts of conspecifics, and therefore ascidian larvae settle preferentially around adult organisms.

The short-distance dispersal of ascidian larvae may be an additional factor leading to the patchy distribution of certain ascidian species, which shape the benthic community structure considerably (Bolker and Pacala 1999). They are able to colonize new settling grounds by their larval dispersal, and because they are fast growing, they often act as pioneer species in the recolonization of seabed regions devastated by iceberg scouring (Gutt and Piepenburg 2003).

The recruitment and settlement patterns influence species distributions over a variety of scales and can vary extremely. Their causes are hard to be determined and may be sometimes just random. The enormous small-scale variability within the transects very likely masked the patterns at the intermediate, and partly also regional scale.

One last factor worth mentioning refers to the atmospheric warming of the Antarctic Peninsula and the resulting environmental changes, primarily the disintegration of ice shelves (Gutt and Piepenburg 2003; Clarke et al. 2009; Barnes and Souster 2011). This process is a potent driver of the benthic communities, since it leads to increased sediment runoff and higher loads of particulate matter (Grebmeier and Barry 1991; Gutt and Piepenburg 2003; Smale and Barnes 2008; Sane et al. 2011; Sahade et al. 2015), which can negatively affect filter-feeding organisms like ascidians. Although no iceberg scours were detected during our study in 2013 in the region off the northern Antarctic Peninsula, other investigations showed that iceberg scouring can change and even destroy entire benthic communities (Jackson 1977; Tatián et al. 1998b). It can also lead to a mosaic of different stages of colonization within a larger shelf region. This mechanism, together with anchor ice formation and other physical factors such as sedimentation and bottom-current patterns, has resulted in the establishment of a highly heterogeneous shelf benthos (Gutt and Piepenburg 2003). Understanding the causes and implications of this variability is particularly important in consideration of climate change, which results in the rapid alteration of marine ecosystems and environments. It is difficult to detect and predict the consequences climate change will have for the ascidian fauna of the Southern Ocean. It is only certain that they are sensible to environmental changes and consequently can serve as a reliable early warning system.

Conclusions

We found that the spatial distribution, abundance and coarse taxon composition of ascidian assemblages off the tip of Antarctic Peninsula largely reflect the different environmental regimes in this region, which are in turn mainly driven by seasonal sea-ice dynamics and oceanographic circulation patterns. Hence, several factors are acting at different scales as ecological drivers of the distribution of the ascidians. The intermediate-scale, primarily depth-related patterns are apparently superimposed by a pronounced small-scale patchiness, which is assumed to be mainly a result of ecological processes, including food supply. Such processes in a region with assumed variable energy limitation are determined by a complex of factors controlling meio-, macro- and megabenthos at different spatial scales. The ecological drivers of small-scale patchiness might therefore be as important as the long-term physiological adaption to a large-scale environment, including its natural variability and biological interactions (Hessler and Jumars 1974; Lampitt et al. 1986). Increasing water temperatures and decreasing sea-ice cover off the Antarctic Peninsula will most likely affect the occurrence and distribution of ascidian species, both directly and indirectly. However, due to the high spatial heterogeneity in the ascidian distribution we need more long-term observations and comparative cause-effect studies to assess in which direction, increasing or decreasing diversity and/or abundance, ascidian assemblages will develop in the future.

References

Anderson MJ (2001) A new method for non-parametric multivariate analysis of variance. Austral Ecol 26:32–46

Anderson MJ, Gorley R, Clarke K (2008) PERMANOVA for PRIMER: guide to software and statistical methods. PRIMER-E Ltd, Plymouth

Arrigo KR, Thomas DN (2004) Large scale importance of sea-ice biology in the Southern Ocean. Antarct Sci 16:471–486

Bakus GJ (1968) Sedimentation and benthic invertebrates of Fanning Island, central Pacific. Mar Geol 6:45–51

Barnes DKA, Souster T (2011) Reduced survival of Antarctic benthos linked to climate-induced iceberg scouring. Nat Clim Chang 7:365–368

Barnes DK, Griffiths HJ, Kaiser S (2009) Geographic range shift responses to climate change by Antarctic benthos: where we should look. Mar Ecol Prog Ser 393:13–26

Bergmann M, Klages M (2012) Increase of litter at the Arctic deep-sea observatory HAUSGARTEN. Mar Poll Bull 64:2734–2741

Bolker BM, Pacala SW (1999) Spatial moment equations for plant competition: understanding spatial strategies and the advantages of short dispersal. Am Nat 153:575–602

Bray JR, Curtis JT (1957) An ordination of the upland forest communities of southern Wisconsin. Ecol Monogr 27:325–349

Burnham KP, Anderson DR (2004) Multimodel inference: understanding AIC and BIC in model selection. Sociol Meth Res 33:261–304

Burrough PA, McDonell RA (1998) Principles of geographical information systems. Oxford University Press, New York

Butman CA (1987) Larval settlement of soft settlement invertebrates: the spatial scales of pattern explained by active habitat selection and the emerging role of hydrodynamical processes. Oceanogr Mar Biol Annu Rev 25:113–165

Cape MR, Vernet M, Kahru M, Spreen G (2014) Polynya dynamics drive primary production in the Larsen A and B embayments following ice shelf collapse. J Geophys Res-Oceans 119: 572–594

Clarke KR (1993) Non-parametric multivariate analyses of changes in community structure. Aust J Ecol 18:117–143

Clarke DB, Ackley SF (1984) Sea-ice structure and biological activity in the Antarctic marginal ice zone. J Geophys Res Oceans 89:2087–2095

Clarke KR, Gorley RN (2006) PRIMER v6: user manual/tutorial. PRIMER-E, Plymouth

Clarke KR, Warwick RM (1994) Change in marine communities: an approach to statistical analysis and interpretation. Natural Environment Research Council, UK

Clarke A, Griffiths HJ, Barnes DK, Meredith MP, Grant SM (2009) Spatial variation in seabed temperatures in the Southern Ocean: implications for benthic ecology and biogeography. J Geophys Res 114:G03003

Cook AJ, Fox AJ, Vaughan DG, Ferrigno JG (2005) Retreating glacier fronts on the Antarctic Peninsula over the past half-century. Science 308:541–544

Davis AR (1987) Variation in recruitment of the subtidal colonial ascidian Podoclavella cylindrica (Quoy & Gaimard): the role of substratum choice and early survival. J Exp Mar Biol Ecol 106:57–71

Davis AD, Butler AJ (1989) Direct observations of larval dispersal in the colonial ascidian Podoclavella moluccensis Sluiter: evidence for closed populations. J Exp Mar Biol Ecol 127: 189–203

Dorschel B, Gutt J, Piepenburg D, Schröder M, Arndt JE (2014) The influence of the geomorphological and sedimentological settings on the distribution of epibenthic assemblages on a flat topped hill on the over-deepened shelf of the western Weddell Sea (Southern Ocean). Biogeosciences 11:3797–3817

Dorschel B, Gutt J, Huhn O, Bracher A, Huntemann M, Huneke W, Gebhardt C, Schröder M, Herr H (2015) Environmental information for a marine ecosystem research approach for the northern Antarctic Peninsula (RV Polarstern expedition PS81, ANT-XXIX/3). Polar Biol. doi:10.1007/s00300-015-1861-2

Ducklow HW, Fraser W, Karl DM, Quetin LB, Ross RM, Smith RC, Stammerjohn SE, Verne M, Daniels RM (2006) Water-column processes in the West Antarctic Peninsula and the Ross Sea: interannual variations and foodweb structure. Deep-Sea Res II 53:834–852

Fischer G, Fütterer D, Gersonde R, Honjo S, Ostermann D, Wefer G (1988) Seasonal variability of particle flux in the Weddell Sea and its relation to ice cover. Nature 335:426–428

Gili JM, Coma R, Orejas C, López-González PJ, Zabala M (2001) Are Antarctic suspension-feeding communities different from those elsewhere in the world. Polar Biol 24:473–485

Grave C (1936) Metamorphosis of ascidian larvae. Carnegie Inst. Washington Paper. Tortugas Lab 29:209–291

Grebmeier JM, Barry JP (1991) The influence of oceanographic processes on pelagic–benthic coupling in polar regions. J Mar Syst 2:495–518

Gutt J (2013) The expedition of the research vessel "Polarstern" to the antarctic in 2013 (ANT-XXIX/3). Ber Polarforsch 665: 1–150

Gutt J, Koltun VM (1995) Sponges of the Lazarev and Weddell Sea, Antarctica: explanations for their patchy occurrence. Antarct Sci 7:227–234

Gutt J, Piepenburg D (1991) Dense aggregations of three deep-sea holothurians in the southern Weddell Sea, Antarctica. Mar Ecol Prog Ser 68:277–285

Gutt J, Piepenburg D (2003) Scale-dependent impact on diversity of Antarctic benthos caused by grounding of icebergs. Mar Ecol Prog Ser 253:77–83

Gutt J, Starmans A (1998) Structure and biodiversity of megabenthos in the Weddell and Lazarev Seas (Antarctica): ecological role of physical parameters and biological interactions. Polar Biol 20:229–247

Gutt J, Starmans A (2003) Patchiness of the megabenthos at small scales: ecological conclusions by examples from polar shelves. Polar Biol 26:276–278

Gutt J, Cape M, Dimmler W, Fillinger L, Isla E, Lieb V, Lundälv T, Pulcher C (2013) Shifts in Antarctic megabenthic structure after ice-shelf disintegration in the Larsen area east of the Antarctic Peninsula. Polar Biol 36:895–906

Hessler RR, Jumars PA (1974) Abyssal community analysis from replicate cores in the central North Pacific. Deep-Sea Res Oceanogr Abstr 3:185–209

Jackson JBC (1977) Competition on marine and hard substrata: the adaptive significance of solitary and colonial strategies. Am Nat 3:743–767

Jackson JBC, Buss L (1975) Alleopathy and spatial competition among coral reef invertebrates. Proc Natl Acad Sci USA 12:5160–5163

Jerosch K, Kuhn G, Krajnik I, Scharf FK, Dorschel B (2015) A geomorphological seabed classification for the Weddell Sea, Antarctica. J Geophys Res. doi:10.1007/s11001-015-9256-x

Keough MJ (1998) Responses of settling invertebrate larvae to the presence of established recruits. J Exp Mar Biol Ecol 231:1–19

Kowalke J (1999) Filtration in antarctic ascidians - striking a balance. J Exp Mar Biol Ecol 242:233–244

Kruskal JB, Wish M (1978) Multidimensional scaling. Sage, Beverly Hills

Lampitt RS, Billett DSM, Rice AL (1986) Biomass of the invertebrate megabenthos from 500 to 4100 m in the northeast Atlantic Ocean. Mar Biol 1:69–81

Lizotte MP (2001) The contribution of sea-ice algae to Antarctic marine primary production. Am Zool 41:57–73

Lockhart SJ, Jones CD (2008) Biogeographic patterns of benthic invertebrate megafauna of shelf areas within the Southern Ocean Atlantic sector. CCAMLR Sci 15:167–192

Maritorena S, d'Andon OHF, Mangin A, Siegel DA (2010) Merged satellite ocean color data products using a bio-optical model: characteristics, benefits and issues. Remote Sens Environ 8: 1791–1804

Millar RH (1960) The identity of the ascidians Styela mammiculata Carlisle and S. clava Herdman. J Mar Biol Ass UK 39:509–511

Moreau S, Mostajir B, Belanger S, Schloss IR, Vancoppenolle M, Demers S, Ferreyra GA (2015) Climate change enhances primary production in the western Antarctic Peninsula. Glob Change Biol 21:2191–2205

Newton KL, Creese B, Raftos D (2007) Spatial patterns of ascidian assemblages on subtidal rocky reefs in the Port Stephens-Great Lakes Marine Park, New South Wales. Mar Freshw Res 58: 843–855

Orsi AH, Whitworth T, Nowlin WD (1995) On the meridional extent and fronts of the Antarctic Circumpolar Current. Deep Sea Res I 42:641–673

Osman RW, Whitlatch RB (1995) The influence of resident adults on recruitment: a comparison to settlement. J Exp Mar Biol Ecol 2:169–198

Peck LS, Clark MS, Morley SA, Massey A, Rossett H (2009) Animal temperature limits and ecological relevance: effects of size, activity and rates of change. Funct Ecol 23:248–256

Petersen JK, Svane IB (1995) Larval dispersal in the ascidian *Ciona intestinalis* (L.). Evidence for a closed population. J Exp Mar Biol Ecol 1:89–102

Piepenburg D, Ambrose WG, Brandt A, Renaud PE, Ahrens MJ, Jensen P (1997) Benthic community patterns reflect water column processes in the Northeast Water polynya (Greenland). J Mar Syst 10:467–482

Primo C, Vázquez E (2007) Zoogeography of the Antarctic ascidian fauna in relation to the sub-Antarctic and South America. Antarct Sci 19:321–336

Primo C, Vázquez E (2009) Antarctic ascidians: an isolated and homogeneous fauna. Polar Res 28:403–414

Primo C, Vázquez E (2014) Ascidian fauna south of the Sub-Tropical Front. In: de Broyer C, Koubbi P, Griffiths HJ, Raymond B, d'Udekem d'Acoz C, Van de Putte AP, Danis B, David B, Grant S, Gutt J, Held C, Hosie G, Huettmann F, Post A, Ropert-Coudert Y (eds) Biogeographic Atlas of the Southern Ocean. SCAR, Cambridge, pp 470–475

Ramirez-Llodra E, Brandt A, Danovaro R, De Mol B, Escobar E, German CR, Levin LA, Martinez Arbizu P, Menot L, Buhl-Mortensen P, Narayanaswamy BE, Smith CR, Tittensor DP, Tyler PA, Vanreusel A, Vecchione M (2010) Deep, diverse and definitely different: unique attributes of the world's largest ecosystem. Biogeosciences 7:2851–2899

Ramos-Esplá AA, Carcel JA, Varela M (2005) Zoogeographical relationships of the littoral ascidiofauna around the Antarctic Peninsula, in the Scotia Arc and in the Magellan region. Sci Mar 69:215–223

Rius M, Branch GM, Griffiths CL, Turon X (2010) Larval settlement behaviour in six gregarious ascidians in relation to adult distribution. Mar Ecol Prog Ser 418:151–163

Sahade R, Tatián M, Kowalke J, Kühne S, Esna GB (1998) Benthic faunal associations on soft substrates at Potter Cove, King George Island, Antarctica. Polar Biol 19:85–91

Sahade R, Lagger C, Torre L, Momo F, Monien P, Schloss I, Barnes DKA, Servetto N, Tarantelli S, Taitán Zamboni N, Abele D (2015) Climate change and glacier retreat drive shifts in an Antarctic benthic ecosystem. Sci Adv. doi:10.1126/sciadv.1500050

Sane E, Isla E, Grémare A, Gutt J, Vétion G, DeMaster DJ (2011) Pigments in sediments beneath recently collapsed ice shelves: the case of Larsen A and B shelves, Antarctic Peninsula. J Sea Res 65:94–102

Segelken-Voigt A, Bracher A, Dorschel B, Gutt J, Huneke W, Link H, Piepenburg D (2015). Spatial distribution patterns of ascidians (Ascidiacea: Tunicata) in combination with information on bathymetry, oceanography, chlorophyll-a, and sea-ice on the continental shelves off the northern Antarctic Peninsula during POLARSTERN cruise ANT-XXIX/3. www.pangaea.de, doi:10.1594/PANGAEA.849291

Shenkar N, Gittenberger A, Lambert G, Rius M, Moreira Da Rocha R, Swalla BJ, Turron X (2015) Ascidiacea World Database. http://www.marinespecies.org/ascidiacea. Accessed at 20 June 2015

Sieg J, Wägele JW (1990) Fauna der Antarktis. Parey, Berlin/Hamburg

Sievers HA (1982) The stratification and water masses at Drake Passage. J Geophys Res 89:10489–10514

Smale DA, Barnes DK (2008) Likely responses of the Antarctic benthos to climate-related changes. Ecography 31:289–305

Smith F, Witman JD (1999) Species diversity in subtidal landscapes: maintenance by physical processes and larval recruitment. Ecology 80:51–69

Smith CR, Mincks SL, DeMaster DJ (2006) A synthesis of bentho-pelagic coupling on the Antarctic shelf: food banks, ecosystem inertia and global climate change. Deep-Sea Res II 53:875–894

Spreen G, Kaleschke L, Heygster G (2008) Sea-ice remote sensing using AMSR-E 89-GHz channels. J Geophys Res 113:C02S03

Starmans A, Gutt J, Arntz WE (1999) Mega-epibenthic communities in Arctic and Antarctic shelf areas. Mar Biol 135:269–280

Strathmann RR, Kendall LR, Marsh AG (2006) Embryonic and larval development of a cold adapted Antarctic ascidian. Polar Biol 29:495–501

Svane I, Havenhand JN (1993) Spawning and dispersal in *Ciona intestinalis* (L.). Mar Ecol 14:53–66

Svane I, Young CM (1989) The ecology and behaviour of ascidian larvae. Oceanogr Mar Biol 27:45–90

Tatián M, Sahade RJ, Doucet ME, Esnal GB (1998a) Some aspects of Antarctic ascidians (Tunicata, Ascidiacea) of Potter Cove, King George Island. Ber Polarforsch 299:113–118

Tatián M, Sahade RJ, Doucet ME, Esnal GB (1998b) Ascidians (Tunicata, Ascidiacea) of Potter Cove, South Shetland Islands, Antarctica. Antarct Sci 10:147–152

Tatián M, Antacli JC, Sahade R (2005) Ascidians (Tunicata, Ascidiacea): species distribution along the Scotia Arc. Sci Mar 69:205–214

Vaughan DG, Marshall GJ, Connolley WM, Parkinson C, Mulvaney R, Hodgson DA, King JC, Pudsey CJ, Tuner J (2003) Recent rapid regional climate warming on the Antarctic Peninsula. Clim Change 60:243–274

Walther GR, Post E, Convey P, Menzel A, Parmesan C, Beebee TJ, Fromentin JM, Hoegh-Guldberg O, Bairlein F (2002) Ecological responses to recent climate change. Nature 416:389–395

Weiss AD (2001) Topographic position and landforms analysis. Poster presentation, ESRI users conference, San Diego, CA. http://www.jennessent.com/downloads/tpi-poster-tnc_18x22.pdf. Accessed 16 Aug 2015

Wienberg C, Wintersteller P, Beuck L, Hebbeln D (2013) Coral Patch seamount (NE Atlantic)—a sedimentological and megafaunal reconnaissance based on video and hydroacoustic surveys. Biogeosciences 10:3421–3443

Wilson MFJ, O'Connell B, Brown C, Guinan JC, Grehan AJ (2007) Multiscale terrain analysis of multibeam bathymetry data for habitat mapping on the continental slope. Mar Geol 30:3–35

Woodin SA (1976) Adult-larval interactions in dense infaunal assemblages: patterns of abundance. J Mar Res 34:25–41

Woodin SA (1978) Refuges, disturbance, and community structure: a marine soft-bottom example. Ecology 59:274–284

Wright DJ, Lundblad ER, Larkin EM, Rinehart RW, Murphy J, Cary-Kothera L, Draganov K (2005) ArcGIS Benthic Terrain Modeler [a collection of tools used with bathymetric data sets to examine the deepwater benthic environment]. Oregon State University, Davey Jones' Locker Seafloor Mapping/Marine GIS Laboratory and NOAA Coastal Services Center

Young CM, Chia FS (1984) Microhabitat-associated variability in survival and growth of subtidal solitary ascidians during the first 21 days after settlement. Mar Biol 81:61–68